SCIENTIFIC REPORTS

OPEN

SUBJECT AREAS:
INFLAMMATION
CELLULAR IMAGING
CELL DEATH IN THE NERVOUS SYSTEM
PARKINSON'S DISEASE

Received
2 October 2012

Accepted
18 October 2012

Published
8 November 2012

Correspondence and requests for materials should be addressed to C.B. (barcia@um.es)

ROCK/Cdc42-mediated microglial motility and gliapse formation lead to phagocytosis of degenerating dopaminergic neurons *in vivo*

Carlos Barcia[1,2], Carmen María Ros[1,2], Valentina Annese[1,2], María Angeles Carrillo-de Sauvage[1,2], Francisco Ros-Bernal[1,2], Aurora Gómez[1,2], José Enrique Yuste[1,2], Carmen María Campuzano[1], Vicente de Pablos[1,2], Emiliano Fernandez-Villalba[1,2] & María Trinidad Herrero[1,2]

[1]Clinical and Experimental Neuroscience, [2]Centro de Investigación Biomédica en Red sobre Enfermedades Neurodegenerativas (CIBERNED), School of Medicine, University of Murcia, Campus de Espinardo, 30071, Murcia, Spain.

The role of microglial motility in the context of adult neurodegeneration is poorly understood. In the present work, we investigated the microanatomical details of microglia-neuron interactions in an experimental mouse model of Parkinson's disease following the intraperitoneal injection of MPTP. The specific intoxication of dopaminergic neurons induces the cellular polarization of microglia, leading to the formation of body-to-body neuron-glia contacts, called gliapses, which precede neuron elimination. Inhibiting ROCK/Cdc42-mediated microglial motility *in vivo* blocks the activating features of microglia, such as increased cell size and number of filopodia and diminishes their phagocyting/secreting domains, as the reduction of the Golgi apparatus and the number of microglia-neuron contacts has shown. High-resolution confocal images and three-dimensional rendering demonstrate that microglia engulf entire neurons at one-to-one ratio, and the microglial cell body participates in the formation of the phagocytic cup, engulfing and eliminating neurons in areas of dopaminergic degeneration in adult mammals.

Microglial cells constitute the first barrier of the innate immune response in the brain and are crucial players in the integrity of the nervous system[1]. Microglia constantly survey the brain parenchyma and are able to detect changes in the tissue and rapidly migrate to damaged areas[2]. The mechanism underlying microglial chemotaxis to areas of degeneration requires the release or leakage of ATP from the injured tissue[3], activating P2Y microglial receptors[4–6]. This signaling is crucial for the microglial migration and invasion. Specifically, $P2Y_{12}$ signals microglial activation[6], while $P2Y_6$ controls phagocytosis[4]. Other compounds, such as the chemokine ligand of CX3CR1, fractalkine, or externalized phosphatidylserine, also play an important role in the interaction of microglial cells toward damaged neurons and, importantly, the balance of the ligand and receptor response might define the final fate of the neurodegenerative process[7–9].

After migration, the microglia repair the tissue through the release of different factors, such as cytokines, trophic factors or neurotrophins, and the removal of debris and undesired elements through phagocytosis[1]. Previous *in vitro* studies performed with fluorescent microspheres, opsonized beads or fluorescently labeled β-amyloid, have shown that microglial cells bind to the prey, forming a phagosome, which fuses with a lysosome to digest the material[10–12]. However, imaging studies concerning the details of microglial phagocytosis *in vivo* are scarce. Time-lapse confocal microscopy studies in zebrafish have demonstrated that microglia phagocytose portions of apoptotic neurons during embryo development *in vivo* through the formation of phagosomes via v0-ATPase a1-mediated mechanisms[13]. In addition, the results of detailed confocal analyses have shown that in the adult hippocampus of mice, the majority of newborn neuroblasts are pruned early during their development through the phagocytosis at microglial filamentous terminals[14]. However, apart from the stages of embryo development[13] and the formation of newborn cells[14], technical limitations have hindered the characterization of the involvement of microglial cells in adult mammalian neurodegenerative diseases *in vivo*. Therefore, understanding the mechanisms of the microglial phagocytosis of degenerating neurons *in vivo* and imaging the details of the microglial cell migration will be a promising area for research.

Cell migration has largely been studied *in vitro*. Motility primarily reflects the dynamic organization of the actin cytoskeleton, and the Rho family of small GTPases (i.e., Rho, Rac and Cdc42) critically regulate this process[15]. Rho maintains stress fibers and focal adhesion[16], while Rac organizes the formation of lamellipodia[17] and Cdc42 promotes the arrangement of filopodia[18–20]. The majority of motile and chemotactic cells such as macrophages and most likely microglia, construct long, thin extensions, called filopodia, which are supported by tight and dynamic bundles of actin filaments[15]. This process also involves the extension of the membrane and filament elongation, which requires the reorganization of the actin cytoskeleton (actin nucleation)[15]. Importantly, for the cells with phagocytic properties, Rho and Cdc42 mediate the reorganization of stress fibers and focal adhesion as well as the rearrangement of filopodia[21,22].

In 1884, E. Metchikoff defined phagocytosis as the cellular engulfment of large particles, particularly those greater than 0.5 μm, which also involves dramatic changes in the shape and movement of the cell. A recent *in vitro* study of macrophages has shown that the process of phagocytosis indeed requires the complex arrangement of the innate immune receptor Dectin-1 at the phagocytic synapse to bind fractions of small pathogens and form a phagocytic cup of approximately 4 μm with a particular microanatomical shape[23]; these results provided insight into the complexity of the engulfing process. Theoretically, microglial cells might also show similar structures during phagocytic clearance in neurodegenerative disorders, but little data have been published regarding these features. For example, it remains unknown whether microglia phagocytose small particles or entire neuronal cell bodies in the neurodegenerative process. In the context of the development of newborn cells, microglial branches phagocytose apoptotic neurons forming "ball-and-chain" structures[14,24]; however microglia might behave differently in the context of neurodegeneration, and the details of amoeboid microglia phagocytosis remain elusive.

After decades of research, the significance of microglial activation in neurodegenerative disorders, such as Parkinson's disease (PD) and Alzheimer's disease[25], is multifaceted, and whether this process exerts a protective or deleterious role remains controversial. To explore the aspects of microglial function in the neurodegenerative process in adult mammals and characterize the mechanisms underlying microglial navigation in the brain parenchyma, we have analyzed the microanatomical details of the process of microglial migration-invasion and phagocytosis *in vivo* using a model of dopaminergic degeneration induced through the specific dopaminergic neurotoxin 1-Methyl-4-phenyl-1,2,3,6-tetrahydropyridine (MPTP). In this study, we observed that microglia polarize toward intoxicated/damaged dopaminergic neurons and establish "gliapses" *in vivo*. The complex intercellular contacts between microglial cells and neurons might represent a crucial aspect of the neurodegenerative scenario. High-resolution confocal analyses and three-dimensional reconstructions of these contacts revealed that the anatomical rearrangement of microglial cells involves the reorganization of the cellular processes, the rearrangement and enlargement of the Golgi apparatus and the nucleation/clustering of the actin cytoskeleton. Importantly, we showed that the blockade of microglial motility, through the inhibition of Rho-associated kinase (ROCK) activity, prevents microglial polarization/migration and the formation of gliapses to protect damaged dopaminergic neurons from elimination. A deeper confocal imaging and 3D rendering revealed that the gliapse formation by microglial cells resolves in a one-to-one phenomenon, phagocyting entire dopaminergic neuronal bodies in the degenerative process. We propose that blocking microglial polarization might preserve degenerating neurons and prevent phagocytosis in PD and other degenerative disorders.

Results

Microglia polarize their processes toward intoxicated/damaged dopaminergic neurons. Microglial cells constantly survey the CNS, moving their processes and renewing their terminal tips to detect changes in the brain parenchyma[2]; therefore, we investigated this phenomenon in a model of adult neurodegeneration *in vivo*. We took advantage of the fact that the pro-neurotoxin MPTP (metabolized to MPP^+) exhibits specific dopaminergic neurotoxicity in the nigostriatal pathway, inducing the particular activation of microglial cells detected in the brain parenchyma (**Fig. 1A, Fig. S1 and Suppl. Movie 1**). In this anatomical area, at 24 h after the injection of MPTP in C57BL6 mice, Iba-1^+ microglial cells showed an activated phenotype characterized by increased cell body size, accompanied by an increase of the number of terminal tips (**Fig. 1B–C**). We hypothesize that this increase of terminals might reflect the migration of microglial cells toward MPP^+-damaged neurons that exert a "find-me" signal to the surrounding environment. Therefore, we used high-resolution confocal microscopy to analyze the physical polarization of microglia in the dopaminergic pathway and measure the number of actual contacts generated between microglial cells and dopaminergic neurons (**Fig. 1D and E**). We observed that the number of contacts between microglia and dopaminergic neurons was significantly increased at 24 h after MPTP inoculation (**Fig. 1E**), suggesting the arrangement of the first stage (24 h) of microglial polarization toward damaged neurons. In addition, at 24 h after MPTP exposure, the surface of contact between microglia and neurons was also measured, and an increase in size was observed upon contact with dopaminergic neurites or dopaminergic cell bodies (**Fig. 1F**). Thus, these observations showed that microglial cells polarize toward MPP^+-damaged dopaminergic neurons, suggesting that the motility and rearrangement of the microglial cytoskeleton occurs concomitantly with microglial activation in neurodegeneration *in vivo*.

Blocking ROCK prevents microglial polarization. The small GTPase ROCK plays a central role in the organization of the cytoskeleton and it is critically involved in the actin rearrangement and the movement of the cell[15]. To determine the role of microglial polarity in dopaminergic neurodegeneration, we used a potent ROCK inhibitor, HA-1077, which has been previously used safely for *in vivo* experiments and in humans to treat several disorders[26]. We did not utilize ROCK knockout mice in these experiments because these mice exhibit severe developmental problems, such as the failed closure of the eyelid and ventral body wall, resulting in open eyes at birth and omphalocele phenotypes in neonates, which die soon after birth[27].

We first analyzed the activity of ROCK using an enzymatic activity assay to measure the phosphorylation of myosin phosphatase target subunit 1 (MYPT-1) at threonine 696 (Thr696) and tested the effectiveness of HA-1077 in the nigrostriatal pathway of C57BL6 mice at 24 h after MPTP administration. We observed that the administration of MPTP significantly increased MYPT-1 phosphorylation in the nigrostriatal pathway (**Fig. 2A**), which is significantly abolished after HA-1077 treatment (**Fig. 2A**). A detailed study of the microanatomy of microglial cells in the nigrostriatal pathway demonstrated that the increase in ROCK activity is associated with the activation of microglial cells, characterized by an increased cell body size, a higher number of processes (**Fig. 2B and C**), and increased expression of F4/80, which is a surface receptor that is augmented during microglial activation in mice (**Fig. S2**). Importantly, the administration of HA-1077 significantly reduced both the microglial cell body size and the formation of the new terminal processes after MPTP administration (**Fig. 2C**). However, HA-1077 did not affect the MPTP-induced increased expression of F4/80; this finding suggests that the expression of F4/80 in microglia after MPTP insult is independent of ROCK-mediated mechanisms (**Fig. S2**). Most importantly, HA-1077 administration completely abolished the formation of MPTP-induced microglial contacts with dopaminergic neurons in the nigrostriatal pathway (**Fig. 2D**), suggesting that

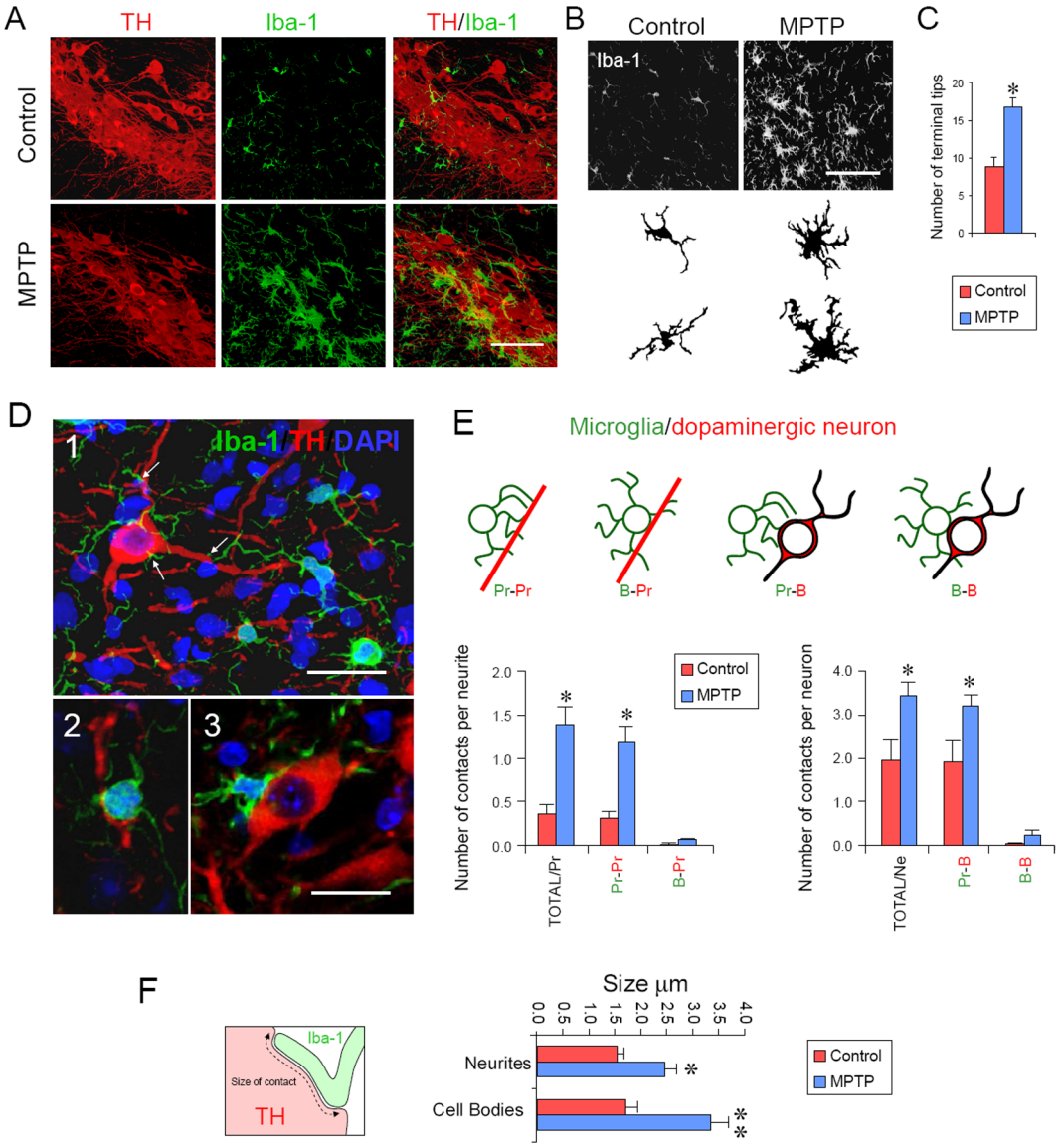

Figure 1 | Microglial cells polarize their processes toward neurons after MPTP. (A) Confocal images of the SNpc show the activation of microglial cells, characterized through the increase of their cell body size and the higher number of terminal tips in close apposition to dopaminergic neurons after MPTP treatment. (B) The confocal pictures from the SNpc were analyzed in detail and representative illustrations of the cells were delineated based on the confocal images. Scale bar in A and B: 50 µm. (C) The number of terminal tips of microglial cells increased after MPTP treatment. *$p<0.05$. (D) Microglial cell processes and cell bodies are in contact with dopaminergic neurites and dopaminergic cell bodies. (D1) Confocal image showing microglial cells (green) contacting their processes with dopaminergic neurons (red). Cell nuclei are counterstained with DAPI (blue). Arrows indicates contacts with dopaminergic cell bodies or neurites. Scale bar in 1: 25 µm. (D2) A microglial cell body in contact with a dopaminergic neurite. (D3) A microglial cell body in contact with a dopaminergic neuron cell body. Scale bar in 3: 20 µm. (E) The number of microglial cells processes in contact with dopaminergic processes [Pr-Pr] and with dopaminergic cell bodies [Pr-B] increases after MPTP treatment. The contacts between microglial cell bodies and dopaminergic structures (B-Pr and B-B) were not modified. (TOTAL/Pr=[Pr−Pr]+[B−Pr]), TOTAL/Ne=[Pr−B]+[B−B]. *$p<0.05$ (F) Quantification of the length of the contact between microglial processes and dopaminergic neurites or dopaminergic cell bodies increases after MPTP treatment. *$p<0.05$, **$p<0.01$.

ROCK might play a critical role in modifying the arrangement of the microglial actin cytoskeleton in neurodegeneration. Based on this observation, we assessed the involvement of Cdc42 as this molecule acts as a center of cell polarity[20], and is intimately associated with the contractility and rearrangement of the actomyosin cytoskeleton and the phosphorylation of MYPT-1 (Thr696)[28]. Western blot analyses of Cdc42 were performed using brain homogenates prepared from MPTP-treated mice. We observed a significant increase of Cdc42 in the nigrostriatal pathway at 24 h after MPTP administration, which was completely reverted after HA-1077 administration (**Fig. 2E and F**), thereby demonstrating the *in vivo* convergence and cooperation of Cdc42 and ROCK signaling in cell invasion and motility, as previously shown *in vitro*[28].

A specific actin cytoskeleton rearrangement is observed in microglia. To further explore the arrangement of the actin cytoskeleton in microglia, sections containing the nigrostriatal pathway were stained with phalloidin to detect F-actin and with an antibody against Cdc42. Because F-actin and Cdc42 are ubiquitously expressed, confocal analyses in single optical sections revealed that all cell types showed phalloidin$^+$ and Cdc42$^+$ staining (**Fig. S3**). Detailed confocal analyses revealed that F-actin and Cdc42 were

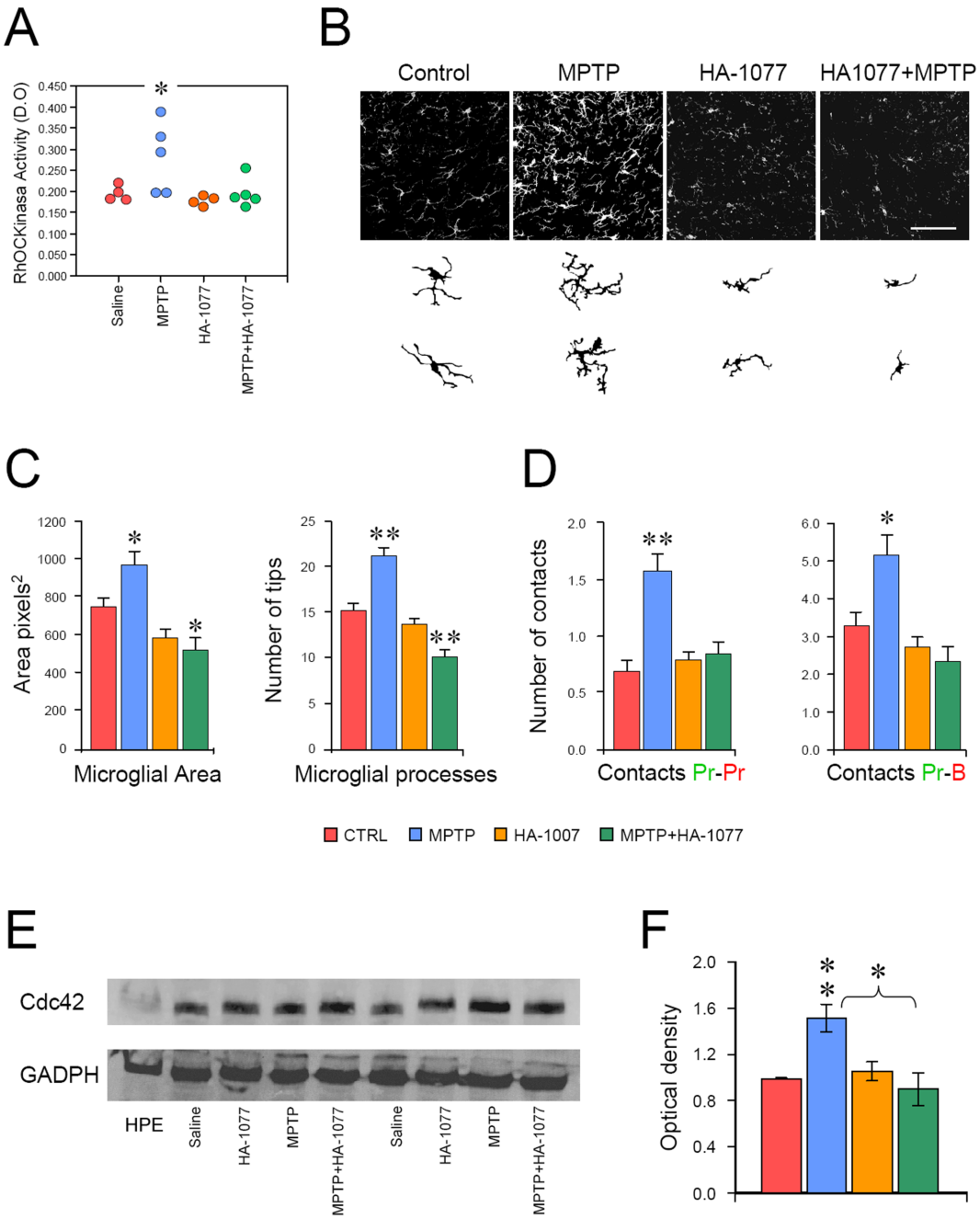

Figure 2 | Blockade of ROCK prevents microglial polarization. (A) HA-1077 inhibits the increase of ROCK activity induced by MPTP. *p<0.05 compared with the control. (B) Top panel shows representative confocal pictures of Iba-1 at the level of the SNpc of the four different groups. Bottom panel shows illustrations of two representative microglial cells from each group obtained from the Iba-1 confocal images. (C) The polarization of microglial cells induced through MPTP treatment is abolished via the specific ROCK inhibitor HA-1077. The increased microglial size and the increased number of microglial processes induced through MPTP treatment are diminished via the specific ROCK inhibitor HA-1077. *p<0.05, **p<0.01 with respect to the control. (D) The increased number of contacts between microglial processes and dopaminergic neurites (Pr-Pr) and cell bodies (Pr-B) induced through MPTP treatment is abolished with specific ROCK inhibitor HA-1077. (E) Western immunoblot of Cdc42 in the nigrostriatal pathway of mice treated with saline, HA-1077, MPTP or MPTP+HA-1077. Human platelet extract (HPE) was used as a control signal for Cdc42. (F) Quantification of the optical density of Cdc42 normalized with GAPDH. Note that HA-1077 inhibits the increase of Cdc42 induced through MPTP treatment, as measured using Western Blot **p<0.01, *p<0.05 compared with the control.

clustered specifically in microglial cells, either in control or Parkinsonian mice, which showed the cytoplasmic accumulation of relative fluorescence compared with surrounding cells (**Fig. 3A, B and Fig. S3**). The clustering and rearrangement of F-actin and Cdc42 in microglial cells are consistent with the constant motility and rapid cytoskeletal rearrangement of these cells during their surveillance of the CNS, as opposed to other cell types, such as astrocytes or neurons, which are slower or almost static[2,29]. However, the confocal analysis of microglial cell interactions with dopaminergic neurons revealed that actin clusters polarize toward the interface of the microglia-neuron contact at the protrusion (**Fig. 3D, D and Fig. S3**). In addition, sections of the nigrostriatal pathway revealed that Cdc42 is also specifically concentrated in the lamiellipodial protrusion (actin-rich lamella) of polarized microglia (**Fig. 3 and Fig. S4**),

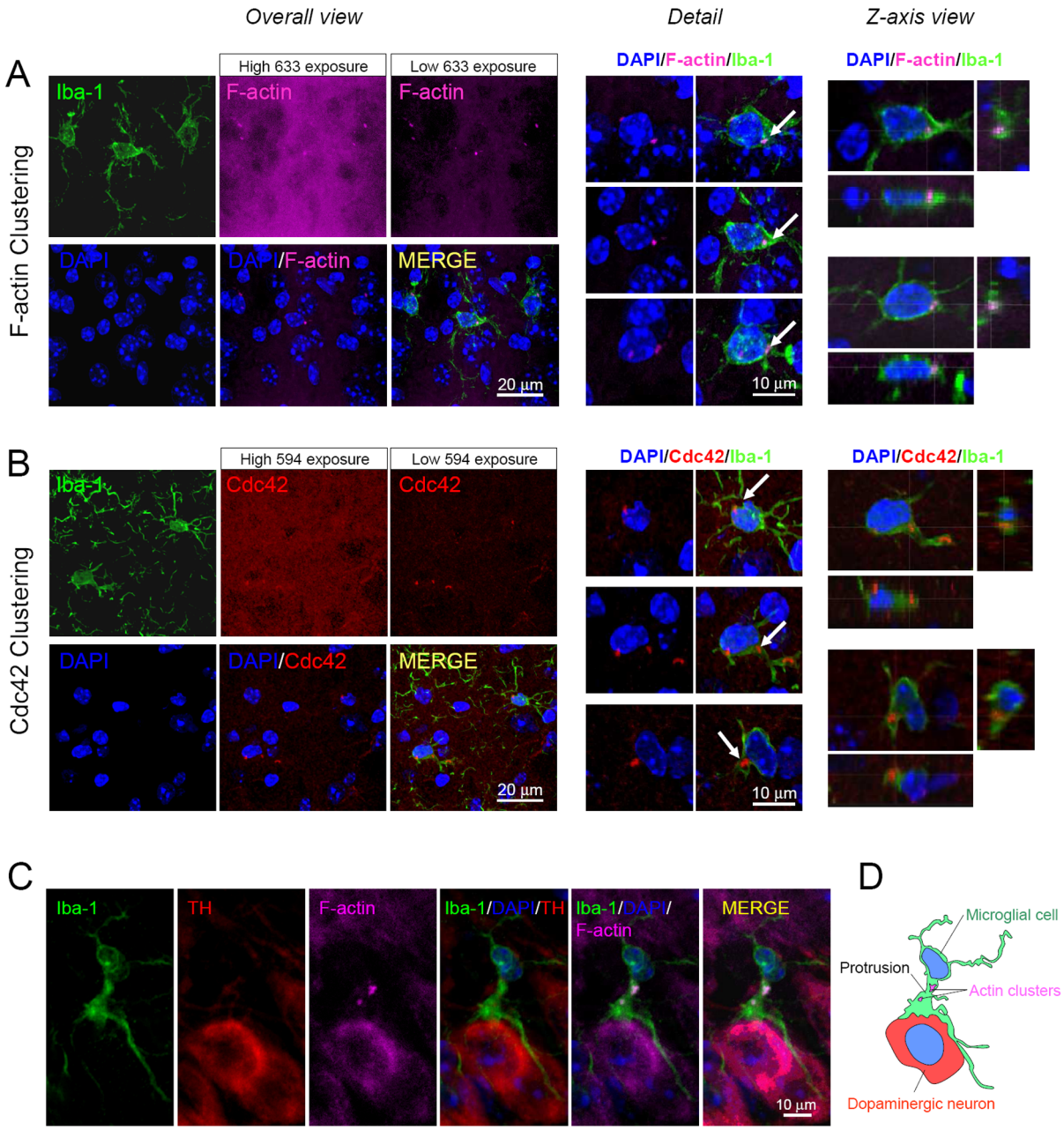

Figure 3 | F-actin and Cdc42 is highly clustered in microglial cells. (A) Stack of confocal sections of the nigrostriatal area immuno-stained for Iba-1 (green), stained with 633-phalloidin (Magenta) to label F-actin, and counterstained with DAPI (blue) in a MPTP-treated mouse. In the *Overall view*, because F-actin is ubiquitous, high exposure to infrared 633-nm laser displays the positive stain of the tissue but hampers the appreciation of details. However, low exposure to the 633-nm laser reduces the intensity of the general F-actin staining and facilitates the appreciation of high fluorescent clusters. Panel on the center shows the *Detail* of these stacks of images. F-actin highly fluorescent clusters are observed in microglial cells but not in the rest of neighboring cells. Panel on the right shows the *Z-axis view*, which facilitates the identification of the specific clustering of F-actin in microglia. (B) Stack of confocal sections of the nigrostriatal area immuno-stained for Iba-1 (green) and Cdc42, and counterstained with DAPI (blue) in an MPTP-treated mouse. In the *Overall view* because Cdc42 is also ubiquitous, high exposure to the 594-nm laser shows the general immuno-staining of the tissue but impedes the appreciation of the details. However, low exposure to the 594-nm laser reduces the intensity of the general Cdc42 staining and facilitates the appreciation of highly fluorescent clusters. The *Detail* of these stacks of images in the central panel shows that Cdc42 highly fluorescent clusters are observed in microglial cells and not in the rest of neighboring cells. The *Z-axis view* on the right panel facilitates the identification of the specific clustering of Cdc42 in microglia. The arrows indicate representative microglial clusters. (C) Confocal analysis of polarization and clustering of F-actin in a microglial cell contacting a dopaminergic neuron after MPTP injection. F-actin cluster appear at the protrusion of polarized microglial cells toward the dopaminergic cell body. (D) Explicative diagram of the image from C.

similar to the clustering of F-actin, as shown above. These observations suggest that HA-1077 blocks the MYPT-1 phosphorylation at Thr696 and might inhibit the process of microglial polarization at the level of ROCK and Cdc42 during lamella formation.

Blocking ROCK prevents neuron elimination and body-to-body (gliapse) formation. To explore the effect of blocking ROCK-dependent microglial polarity on neuronal degeneration, we performed an MPTP intoxication experiment in mice sacrificed at

three different time windows (24, 48 and 72 h after MPTP) to observe a quantifiable and evident neuronal death after the administration of MPTP. Importantly, we observed that blocking ROCK through HA-1077 administration prevents MPTP-induced neuronal degeneration, as measured by the quantification of TH^+ and $Nissl^+$ neurons, indicating that ROCK-mediated microglial cell polarity *in vivo* might be necessary for neuron elimination (**Fig. 4A, B and Fig. S5A**).

The detailed analysis of the microglia-neuron contacts at these time points revealed an increase of the "microglial cell body-neuronal cell body" contacts that precede neuron degeneration, suggesting that this contact might be critical for neuronal elimination (**Fig. 4C and D**). Interestingly, the number of one-to-one body-to-body contacts increased nearly 0.2, indicating that 20% of the dopaminergic neurons showed gliapses at 48 h after MPTP treatment. This percentage is consistent with the amount of dopaminergic neuronal loss observed at 72 h, which is nearly 25% of the dopaminergic neuronal loss compared with the control. Moreover, to exclude the possibility that the preservation of SNpc dopaminergic neurons does not reflect the absence or decrease of MPP^+ in the nigrostriatal pathway, HPLC was used to measure MPP^+ showing that HA-1077 administration does not impede the entrance of MPP^+ into the dopaminergic pathway (**Fig. S5B**).

Micro-anatomical analysis reveals the phagocytic character of Gliapses. A microanatomical analysis of the neuron-microglia body-to-body contacts after MPTP administration revealed immunological synapse-like structures between the microglia and neuron, herein referred to as "gliapses", which represent a new concept based on the anatomical relationship between glial cells and neurons that was originally described in the electrophysiological context of neurotransmission[30]. The anatomical body-to-body engagements (gliapses) between microglia and dopaminergic neurons that we observed after MPTP treatment share some elements with T cell-APC immunological synapses. Three-dimensional reconstructions of the captured stacks of images revealed that one of the key features of these engulfing gliapses, which represents the flat interface between the two cell bodies, is a structure reminiscent of lymphocyte-target cell immunological synapse (**Fig. 5**). However, in contrast to lymphocytes, the microglial cells presented long thin filopodial processes, which participate in gliapse formation and frequently embrace the neuronal cell bodies after MPTP (**Fig. 5A–D**). In addition, these microglial processes are reduced in number or completely absent from the side of the cell that was not in apposition to the neuron cell body, and most microglial processes were polarized, contacting the neuronal cell body (**Fig. 5B and D**). In addition, confocal three-dimensional rendering showed that the

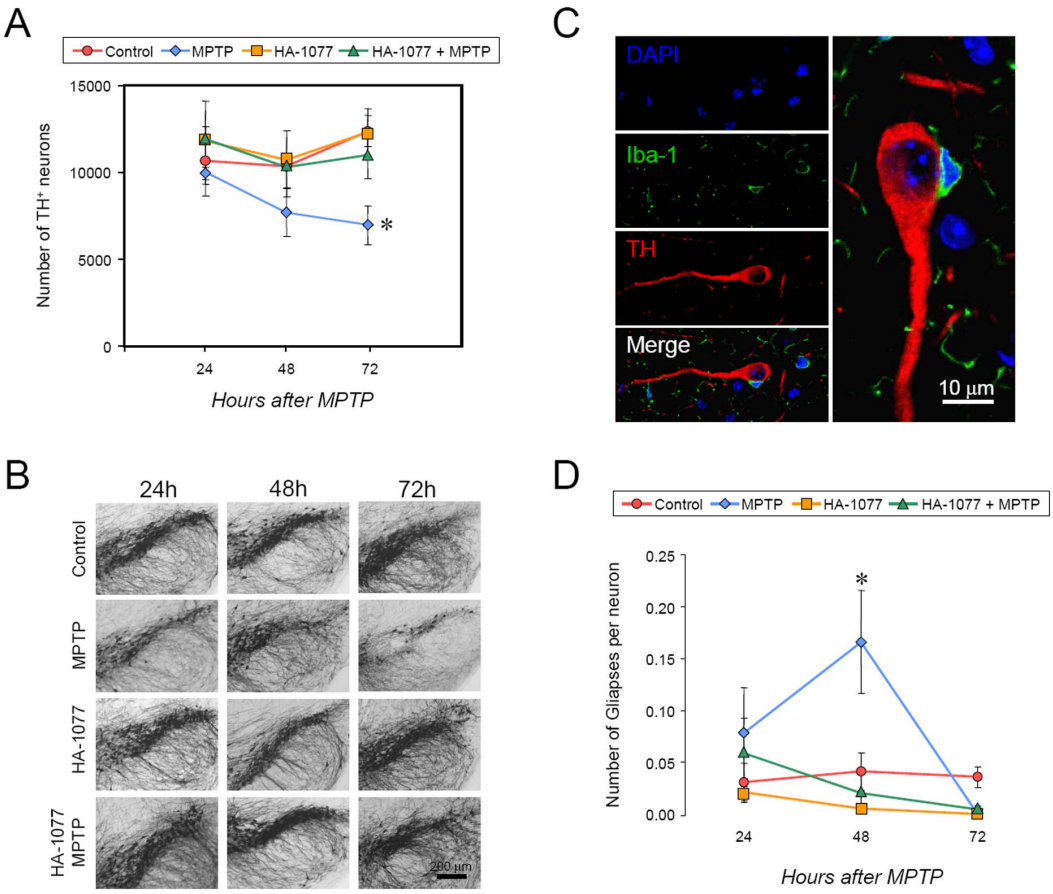

Figure 4 | HA-1077 treatment prevents gliaptic body-to-body contacts and neuron elimination. (A) Quantification of the number of dopaminergic neurons of the SNpc of mice treated with Saline (Control), MPTP, HA-1077 or MPTP + HA-1077. The treatment with HA-1077 prevents the dopaminergic degeneration induced by MPTP. (B) Representative images of immuno-staining for TH^+ neurons to observe dopaminergic neurons of the SNpc of a representative mouse of each experimental group analyzed. (C) Illustration of a characteristic gliaptic body-to-body contact between microglia and TH neurons. The augmented detail of the merged image is shown rotated in the vertical picture. (D) Quantification of the number of body-to-body contacts between dopaminergic neurons and microglial cells of the SNpc of mice treated with Saline (Control), MPTP, HA-1077 or MPTP+HA-1077. The formation of body-to-body contacts precedes neuronal degeneration and conversely treatment with HA-1077 prevents the formation of body-to-body contacts after MPTP treatment.

Golgi apparatus was also polarized at the interface, suggesting secretory or phagocytic domains of these gliapses (**Fig. 5E and F**). Because the size of the Golgi apparatus fluctuates with secretory and phagocytic activity, we also measured the size of the Golgi apparatus in the microglia from mice after MPTP treatment in the SNpc. We observed that the size of microglial Golgi increases after exposure to MPTP, an effect that is indeed reversed with ROCK inhibition (**Fig. S6**).

Importantly, evidence from captured images and 3D rendering show that microglial cells engulf entire neuronal bodies, showing a clear phagocytic appearance (**Fig. 6A, images 1, 1′, 2, 2′ and Suppl. Movie 2**). In these events, the TH labeling is weak where microglial cells surround a big percentage or the entire dopaminergic cell body; the neuronal cell body becomes smaller (**Fig. S7**), and the nucleus appears condensed, suggesting that these gliapses might become phagocytic synapses (**Fig. 6A, images 2 and 2′**). Importantly, a further detailed micro-anatomical analysis showed frequent and striking structures, which are only present in the SNpc after MPTP administration and were not detected in the rest of the dopaminergic pathway (**Suppl. Movies 3a and 3b**). Single microglial cells frequently appear surrounding an extra nucleus, which presents pycnotic features, such as the condensation or fragmentation of chromatin (**Fig. 6A, images 3 and 3′, B–D, Fig. S8 and Suppl. Movie 4**). This engulfed extra nucleus is located in an "Iba-1 negative space", with the appearance of a microglial endosome, suggesting the formation of a microglial phagosome engulfing a dopaminergic neuron (**Fig. 6D and E and Suppl. Movies 5a, 5b and 6**). To demonstrate the phagocytic character of this microglial cells, we stained these structures with antibodies against Cathepsin-D, which specifically localizes to lysosomes. We observed Cathepsin-D^{+} lysosomes in microglial cells consistently localized in the vicinity of the microglial nucleus in proximity to phagosomes containing the extra nucleus (**Fig. 7A–E**); this finding suggests that this giant phagosome might be eliminated through phagocytic microglia via the formation of smaller phagolysosomes. To further explore the state of actin in this phagocytic state, we also stained brain sections with phalloidin and observed a clear clustering of F-actin near the microglial nucleus in all cases (**Fig. 8A–B and Suppl. Movie 7**). However, the orientation of the F-actin accumulation was variable (**Fig. 8**) and did not have a clear polarization. Although the clustering of F-actin is maintained in the engulfing process, it appears to migrate away from the interface between the microglial nucleus and the giant phagosome.

Discussion

In the present work, we showed that microglial cells polarize and contact MPP^{+}-damaged dopaminergic neurons, forming complex intercellular appositions, gliapses, that lead to the phagocytosis of dopaminergic cell bodies. This process of cellular invasion/migration is ROCK-dependent and involves the actin cytoskeleton; importantly, the inhibition of this process prevents the elimination of

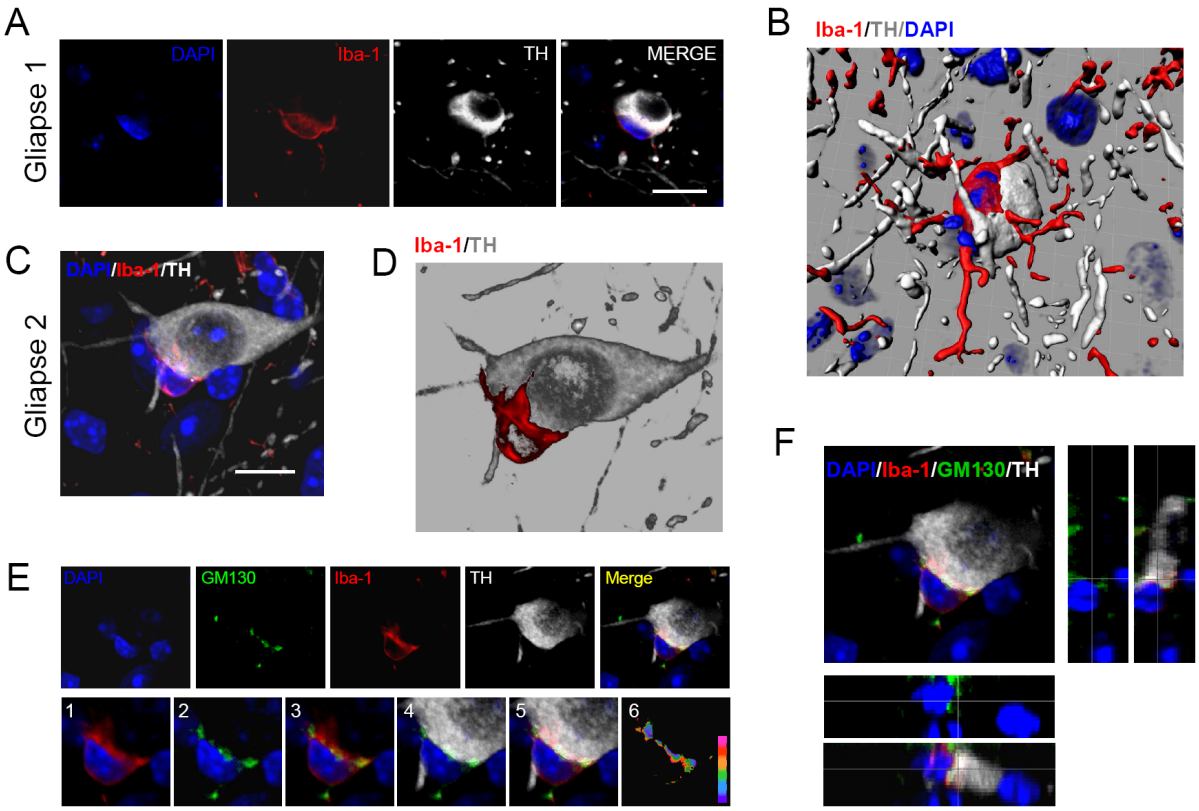

Figure 5 | Microanatomy of engulfing gliapses formation in the SNpc of Parkinsonian mice. (A) Image of a gliapse in the SNpc of an MPTP-treated mouse (Giapse 1). The microglial cell (red) is in close apposition with a dopaminergic neuron (white) and its processes are polarized to the dopaminergic neuron cell body. (B) Three-dimensional rendering of Gliapse 1. (C) Image of gliapse formation in the SNpc of an MPTP-treated mouse. (D) Three dimensional rendering of Gliapse 2. (E) Analysis of polarization of Golgi and Iba-1 at the engulfing gliapse. Optical sections (0.5 μm thick) from Gliapse 2 are shown in the top row. Immunofluorescence for the Golgi apparatus (GM130, green), microglia (red) and TH (white) are displayed, together with nuclear counterstaining using DAPI (blue). GM130 is arranged at the interface. The bottom row shows the details of the interface area. Iba-1 appears polarized toward the dopaminergic neuron (1). Microglial GM130 is polarized only on the side of the cell in contact with the dopaminergic neuron (2, 3). GM130 occupies the area of the intercellular interface (4, 5). Ratio of the physiological activity analysis of the channels shows the maximum activity at the engulfing gliapses interface (6). (F) Confocal analysis of the polarization of Golgi in the xy plane and along the z-axis. Polarization of GM130 can be observed in the lateral views along the z-axis scanning. Scale bar in A; 25 μm, in B; 15 μm.

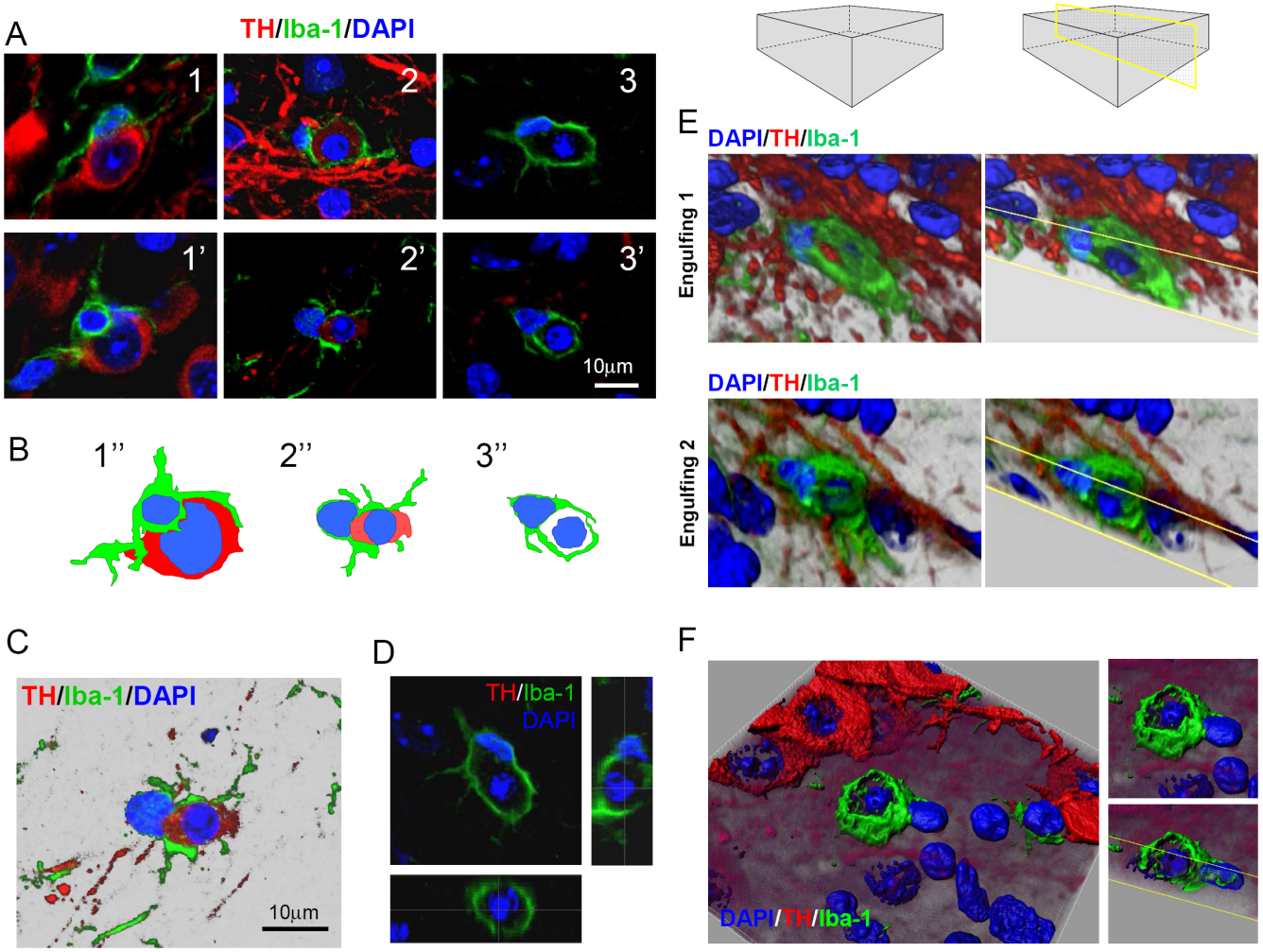

Figure 6 | Microglial cells phagocyte degenerating neurons in the SNpc (A) Confocal images of engulfing events in the SNpc of mice after MPTP-treatment. Microglial processes engulfing a dopaminergic neuron after MPTP treatment (1, 1′, 2, 2′). Engulfed dopaminergic neurons present a smaller size, low intensity of TH and pycnotic nuclei (2, 2′). Microglial cells engulfing pycnotic nuclei (3, 3′). (B) Diagrams of the three events described in A (1″, 2″ and 3″). (C) The subtraction of the black background in the engulfing gliapse shown in 2 and 2″ facilitates the observation of the pycnotic nature of the nucleus of the neuron, the punctuated TH staining and the shape of the engulfed dopaminergic neuron. (D) Lateral view of the z-axis of an engulfing microglia. Note that the pycnotic extra nucleus is completely surrounded by the Iba-1$^+$ membrane. (E) Three-dimensional reconstructions of engulfing microglial cells in the SNpc after MPTP treatment. In both examples, the extra nucleus is completely surrounded by the membrane of the microglial cell. The clipping plane (yellow) is shown at the level of the extra nucleus. (F) Overhead view of a three-dimensional reconstruction of a microglial cell engulfing an extra nucleus in the SNpc of a mouse after MPTP treatment in the SNpc.

dopaminergic neurons. Our high-resolution images showed that the entire microglial cell body participates in the formation of the phagocytic cup differently from the smaller phagocytic cups formed in the engulfing of small pathogens[23] and differently from the elimination of newborn cells in which only the microglial branches are involved in the phagocytic process, forming a ball-and-chain structure[14]. In our model, phagocytosis is a one-to-one process and the microglial cell body apposes the neural cell body with its processes oriented toward the neuron. The engulfing microglia forms a giant phagosome (20 μm diameter) containing a single neuron, with clear pycnotic characteristics, and contains Cathepsin-D$^+$ lysosomes in well-determined areas of the microglial cytoplasm, indicating active phagocytosis.

It is reasonable to propose that microglia cells send "find-me" and "eat-me" signals, which might be ATP-dependent, involving P2Y receptors during the first stages of polarization, as has previously established[4,6]. In addition, it is likely that the secretion or leakage of ATP might be a sufficient stimulus to direct microglial cells toward damaged neurons, activating ROCK signaling and initiating movement and polarization. We showed that ROCK signaling involves the phosphorylation of MYPT-1 at Thr696 *in vivo*, as demonstrated using an enzymatic activity assay, and this phosphorylation is associated with the Cdc42 cascade, which shares the same domains in cell polarization and actin cytoskeleton rearrangement[28].

Importantly, our study demonstrates that ROCK inhibition diminishes most microglial activation properties, such as the increased cell body size, number of filopodial processes and size of Golgi apparatus, after MPTP insult. In contrast, ROCK inhibition does not reduce the MPTP-induced increase of F4/80 expression in microglial cells, suggesting that this latter feature of microglial activation is independent of ROCK-mediated mechanisms, indicating that microglial cells receive activation signals from the MPP$^+$-damaged neurons and consequently over-express F4/80, even when their motility is blocked by HA-1077. This observation is consistent with previous studies performed in F4/80 knockout mice, where the motility and distribution of the macrophages in the organism remained unaffected, while the recognition of pathogens and the induction of antigen-specific efference was markedly altered[31]. These results show

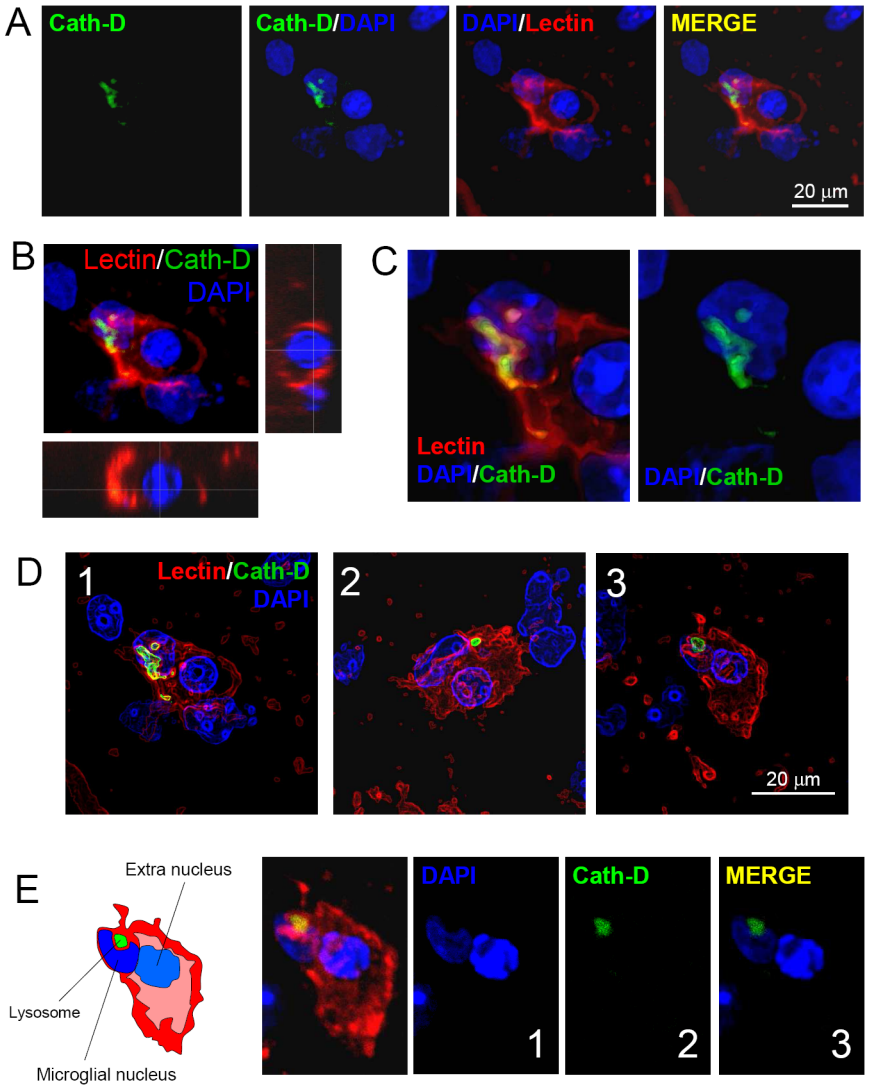

Figure 7 | Localization of lysosomes in engulfing microglia. (A) Confocal analysis of an engulfing microglial cell stained with Lectin (red), showing Cathepsin-D$^+$ lysosomes (green) in the SNpc of a mouse treated with MPTP. DAPI (blue) was used as a counterstaining. (B) Lateral view of the extra-nucleus inside the microglial phagosome from A. (C) Detail of Cathepsin-D$^+$ lysosomes close to the microglial nucleus. The images were treated with a surface filter to better appreciate the cellular structures. (D) Examples of engulfing microglia with Cathepsin-D$^+$ lysosomes. An image filter was applied to highlight the contours in the three examples. (E) Detailed confocal analysis of an engulfing microglia showing a kidney-shaped nucleus surrounding the Cathepsin-D lysosome. The pycnotic engulfed extra nucleus can also be clearly observed with the DAPI counterstaining.

that motility and F4/80 expression are two independent pathways in the process of macrophage/microglia activation.

According to our results, the process of microglial polarization in dopaminergic neurodegeneration undergoes different steps in adult mice, beginning with the polarization of filopodial processes toward neurons (occurring at 24 h after MPTP treatment), followed by the polarization/migration of the microglial cellular body (occurring 48 h after MPTP). These data illustrate the velocity of the approach of the microglial cell to the damaged dopaminergic neuron after MPTP administration, which suggests that microglial cells might have a specific time window, within 24 h, to recognize the state of the neuron and "decide" and resolve its final fate. Importantly, our data show that body-to-body (**B-B**) contacts are increased at 48 h after MPTP and precede the neuron elimination observed at 72 h, suggesting that the elimination of dopaminergic neurons requires prior gliapse formation followed via microglial phagocytosis.

Our images show that microglial cells engulf cells with clear pycnotic nuclei and an apoptotic appearance. The time-frame quantifications suggest that microglial cells pursue degenerating neurons and digest entire cell bodies during MPP$^+$-induced damage is ongoing. Gliapse body-to-body formation precedes neuron elimination and does not take place at 72 h after the MPTP administration, suggesting that the degenerating process is resolved during this time frame. Although in our model we are certain that MPP$^+$ is the primary cause of the dopaminergic neurotoxicity, the engulfing process might also influence the neuronal degeneration and the apoptotic and condensed appearance of the nuclei. Recent data demonstrate that phagocytosis alone induces cell death. New reports have provided evidence that microglial phagocytosis might be a phenomenon for the induction of neuronal death[32] and promotion of apoptotic cell corpse degradation[33]; thus, in our scenario, the occurrence of the two phenomena as well as the toxicity of MPP$^+$ and active phagocytosis might all participate in dopaminergic body degradation and the formation of the pycnotic nuclei.

Other cells from the blood stream could infiltrate the brain parenchyma to repair the tissue damage. Peripheral monocytes/macrophages infiltrate from the blood stream to the brain parenchyma. Previous studies have shown that, in similar protocols of acute

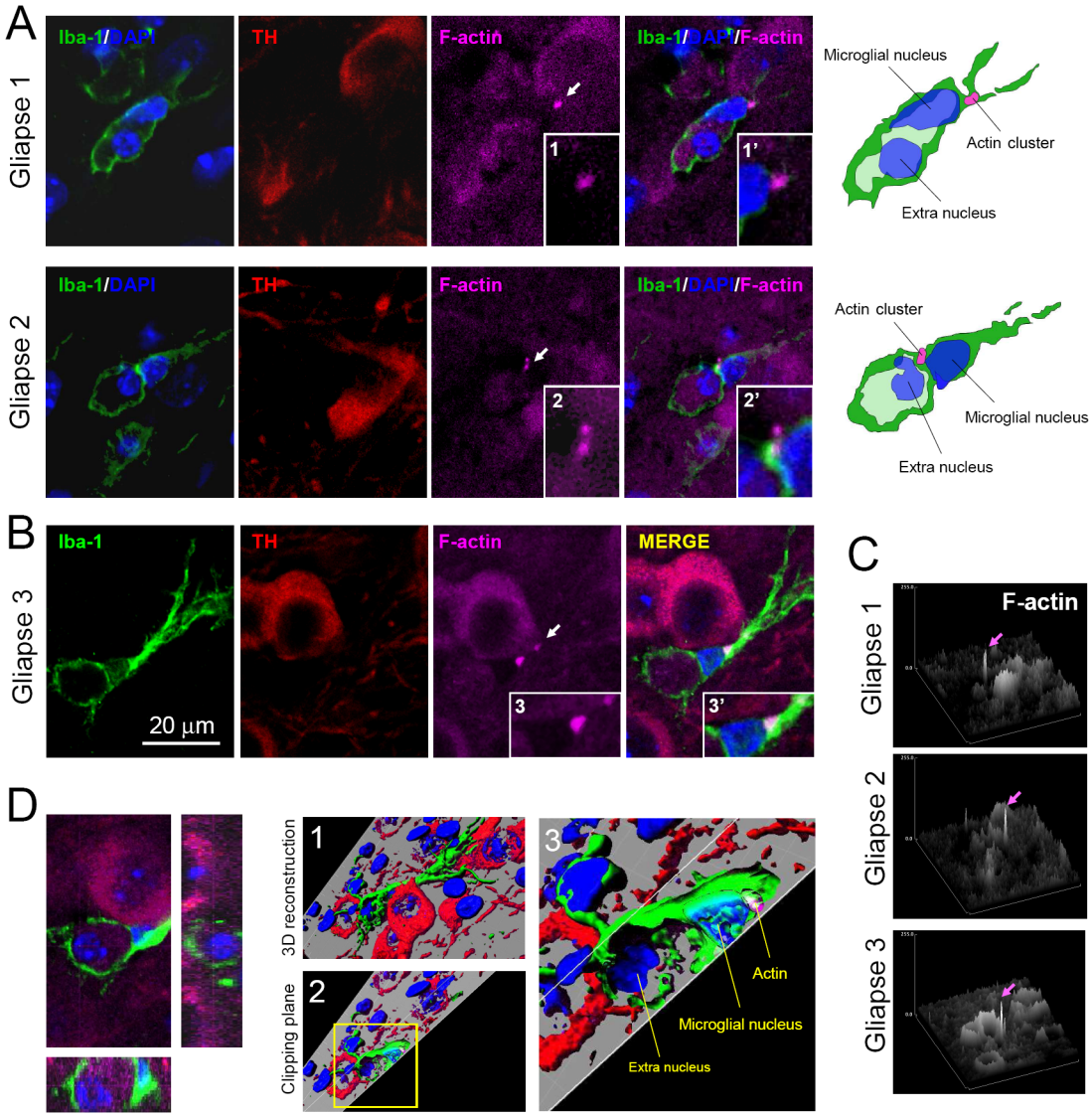

Figure 8 | Actin clustering in engulfing microglia. (A) F-Actin accumulation can be observed in the vicinity of microglial nucleus in engulfing gliapses in the SNpc of Parkisonian mice. Two examples of gliapses are shown, where a microglial cell engulfs an extra nucleus and shows F-actin accumulation (arrows). Higher magnifications of the F-actin accumulation are shown in 1, 1′, 2 and 2′. Explicative diagrams are shown on the right. (B) Example of F-actin accumulation in other engulfing gliapse. Higher magnifications of the F-actin accumulation are shown in 3 and 3′. In this case, the extra nucleus is located at a different optical plane and the lateral view along the z-axis is shown in D. In all three gliapses actin clusters are moved away from the interface phagosome-microglial nucleus. (C) The 3D analysis of the level of relative fluorescence of F-actin in the three gliapses studied. The maximum level of F-actin fluorescence was detected specifically in the engulfing gliapses (magenta arrows). (D) Lateral z-axis view and three-dimensional reconstruction of *Gliapse 3*. Overview of the 3D reconstruction is shown in 1. The clipping plane at the level of F-actin accumulation of the 3D reconstruction is shown in 2. The yellow insert in 2 is magnified in 3.

parkinsonization, MPTP administration does not initially increase, but rather paradoxically, decreases, specific macrophage infiltration in the SNpc[34]. However, the results of long-term experiments with MPTP administration have shown that infiltrated monocytes might present microglial phenotype and express microglial markers in the SNpc several weeks (60 days) after the initial MPTP inoculation but not in the early days after the parkinsonization[35]. These results clarify that the process observed in the present study, within 72 h, is most likely performed through resident microglia and not other infiltrated monocytes or macrophages.

Theoretically, the phagocytosis performed through healthy microglia is a necessary and beneficial process to isolate a dead neuronal cell body and avoid tissue damage that might cause in the parenchyma. Therefore, on one hand, the use of ROCK inhibitors as a therapeutic tool might apparently represent a problem because the consequences of keeping non-phagocytosed MPP^+-damaged dopaminergic neurons remain unknown, and their long-term physiological functionality might be questioned. However, on the other hand, increasing evidence has shown that microglia might be inappropriately active in PD patients, and therefore blocking microglial cell activity could be beneficial. Indeed, previous studies have shown that microglia phagocytose viable neurons in a neuro-inflammatory environment and induce apoptosis[9,32], suggesting that phagocytosis might be an important factor for the understanding of the neurodegeneration of PD. In addition, dopaminergic neurons are especially vulnerable to inflammation, and these responses might be crucial in aggravating dopaminergic degeneration in the SNpc[36]. In fact, recent findings have demonstrated that human leukocyte antigen complex-DR (HLA-DR) gene polymorphisms are linked to the late onset idiopathic PD, suggesting an inflammation-related origin

of the disease involving microglia[37]. Precisely, HLA-DR is the same antigen that is over-expressed in activated microglial cells in PD[25] and MPTP-intoxicated humans[38] and non-human primates[39]. Consistent with this notion, glial-mediated sustained neuro-inflammation might be harmful for the surrounding parenchyma, and the putative negative effect of microglia in PD, might exacerbate the pro-inflammatory response and an overly activated phagocytic arm. Therefore, treatment with anti-inflammatory drugs has been suggested as a preventive therapy for neurodegeneration[40]. Indeed, blocking motility through ROCK inhibitors might represent a potential strategy to diminish microglial-mediated inflammatory responses, specifically preserving neurons from microglial phagocytosis and therefore preventing their complete elimination. Importantly, because microglial activation is aggressively initiated in early PD[41] but remains stable for years[42], it is essential to consider that treatment with ROCK inhibitors might be relevant in the first stages of the disease to prevent glial-mediated inflammation and neuronal elimination.

In conclusion, in the context of neurodegeneration, where the phagocytic domain might be exacerbated, microglia could also eliminate neurons unnecessarily and create a pathological environment in which blocking reactive microglia with ROCK inhibitors could be justified and beneficial, at least to preserve neurons from phagocytic elimination. ROCK inhibitors might be a promising alternative for the treatment of some neurodegenerative diseases, such as PD[26], and further basic and clinical research is needed to enhance the current understanding of the function of microglia and inflammation in both experimental models and patients to evaluate the therapeutic benefits and determine the favorable targets to administer effective disease-modifying drugs.

Methods

MPTP mice and ROCK inhibitor treatment. Adult male mice C57BL/6J (ten weeks old) were purchased at Jax®Mice (The Jackson Laboratory, Bar Harbor, Maine USA) and housed in a special room under adequate temperature (21°C) and 12 hour day-night cycles. The mice were injected (via intraperitoneal injection) either with a single dose of 1-Methyl-4-phenyl-1,2,3,6-tetrahydropyridine (MPTP) hydrochloride (Sigma-Aldrich) (20 mg/Kg) dissolved in saline, or the same volume of saline, or the ROCK inhibitor HA-1077 (Sigma-Aldrich), or a combination of HA-1077 + MPTP, and sacrificed at 24, 48 or 72 h after the single dose (at least n=5 per group). HA-1077 was also dissolved in saline and injected intraperitoneally in a single dose (40 mg/Kg) at 30 minutes prior to MPTP administration. All mentioned studies performed in mice were conducted in accordance with the regulations of the state members of the European Union (2003/65/CE), the Guidelines of the European Convention for the protection of Vertebrate Animals used for Experimental and other scientific purposes of the Council of Europe (no. 123, June 15th, 2006), the European Communities Council Directive 2010/63/ECC, and the National Institutes of Health Guide for the Care and Use of Laboratory Animals (NIH Guide, revised 1996). In addition, the Committee of Ethics of the University of Murcia approved the protocols and experiments described in the project SAF2010-21274.

Western immunoblot. *Primary antibodies.* To asses changes in Cdc42 in the nigrostriatal pathway of mice a western immunoblot was performed with anti-Cdc42 diluted 1 : 500 (Cytoskeleton, Denver, CO, USA). The GAPDH antibody was used to determine the housekeeping of each sample (mouse anti-GAPDH, 1 : 500, Chemicon, Temecula, CA, USA).

Preparation of tissue extracts. C57BL6 mice were injected either with saline (n=5), MPTP (n=5), HA-1077 (n=5) or MPTP+HA-1077 (n=5), according to the protocol described above. At 24 h after the treatment, the mice were sacrificed through cervical dislocation. The brains were quickly harvested on ice, frozen and cut into 1-mm-thick sections with the aid of a matrix for brain slicing. The striatum and the Substantia Nigra *pars compacta* (SNpc) were dissected according to the appropriate coordinates in the mouse brain atlas[43] using a punching device (Harvard apparatus, Harvard bioscience company) with a 1-mm internal diameter and a thin needle, respectively. The tissues were immediately homogenized using a disposable pellet pestle (Sigma-Aldrich, St. Louis, MO, USA) in RIPA buffer, containing 50 mM Tris/HCl pH 7.6, 150 mM NaCl, 1 mM EDTA, 1% SDS, 1% Triton X-100, a 1X cocktail inhibitor (Sigma-Aldrich, St. Louis, MO, USA), 1 mM PMSF, 0.2 mM Na_3VO_4 and 1 mM NaF. After centrifugation (15,000Xg for 15 minutes at 4°C), a sample of the supernatant was analyzed to determine the total concentration of the protein in the sample using the Micro BCA kit (Pierce, Rockford, IL, USA). Other aliquots of the samples were mixed with 4x reducing loading buffer (200 mM Tris/HCl pH 6.8, 4% SDS, 30% glycerol, 4% β-mercaptoethanol, 4% blue bromophenol), boiled for 3 minutes and stored at -20°C until further use.

Electrophoresis and immunoblotting. For each sample, 80 μg of proteins was separated in a 12% SDS-polyacrylamide gel. The molecular mass standard (ColorBurst©, Sigma-Aldrich, St. Louis, MO, USA) containing precisely sized recombinant proteins of 210, 90, 65, 40, 30, 20, 13, 8 kDa, human platelet extract as a control for Cdc42 signal (40 μg) (Cytoskeleton, Inc.), and the samples of the nigrostriatal pathway were run on the same gel and transferred onto a nitrocellulose membrane. The samples were run at constant voltage (200 mV) at room temperature (RT) for 1 hour. After electrophoresis, the protein samples were transferred onto a nitrocellulose membrane using a transfer buffer (25 mM Tris/HCl, 192 mM glycine, 0.1% SDS, 20% methanol). Ponceau S staining (Bio-Rad, Hercules, CA, USA) was used to verify equal protein loading in all the lanes. Non-specific biding sites were blocked upon incubation in 5% dry milk diluted in 1X TTBS (20 mM tris/HCl pH 7.5, 500 mM NaCl, 0.05% tween-20) for 2 h at RT. The membranes were incubated overnight at 4°C in primary antibody diluted in 3% BSA, 0.05% NaN_3, in 1X TTBS. After rinsing twice with 1X TTBS and 3 times with 2.5% dry milk in 1X TTBS, the membranes were incubated for 1 h at RT in ECL sheep anti mouse IgG, horseradish peroxidase conjugated secondary antibody (Amersham, GE healthcare, Little Chalfont, Buckinghamshire, UK) diluted 1 : 5,000 in 2.5% dry milk in 1X TTBS. The antibody binding sites were revealed using the ECL Plus Western Blotting Detection System (Amersham, GE healthcare, Little Chalfont, Buckinghamshire, UK).

The intensity of the bands was evaluated through densitometry analysis using ImageJ 1.41 software. The optical density of each protein band was normalized against the optical density of the GAPDH band, used as internal standard, in the same lane. For each independent experiment the differences between the experimental groups were expressed as treated/ctrl. The graphs represent the average of the ratios calculated from five independent experiments ± SEM. A One-Way ANOVA Duncan test was used to determine the p value. Differences were considered significant when $p \leq 0.05$.

RhO-associated kinase (ROCK) Activity Assay. C57BL6 mice were injected either with saline (n=5), MPTP (n=5), HA-1077 (n=5) or MPTP+HA-1077 (n=5), according to the protocol described above and following the same procedure of tissue extract described for western immunoblot analysis. The ROCK activity was analyzed using a 96-well ROCK activity assay kit (Cell Biolabs, INC., CA, USA). The experiments were performed according to the manufacturer's protocol, using 10 ml of protein lysate. The total starting protein concentration for every sample was 1 mg/ml. The activity of ROCK was measured by quantifying the level of phosphorylation of MYPT-1 in Thr696. Briefly brain lysates were placed in MYPT-1-coated wells and incubated during 60 minutes at 30°C. After washing, incubation of anti-Phospho-MYPT-1 (Thr696) antibody was conducted for 1 h. After washing, the HRP-conjugated secondary antibody was added. After a 1-hour incubation, the plates were washed, and the substrate solution was added for 10 minutes and the OD was read in a microplate reader capable of reading at 450 nm (620 nm was used as reference wave length).

Tissue and specific staining. *Mice.* C57BL6 mice were injected either with saline (n=15), MPTP (n=15), HA-1077 (n=15) or MPTP+HA-1077 (n=15), according to the protocol described above. One, two or three days after MPTP injection, mice (n=5 per group and time point) were anesthetized i.p. with an overdose of Ketamine (50 mg/kg) and Xylazine (50 mg/kg) and perfused-fixed with oxygenated Tyrode's solution followed by 4% paraformaldehyde in PBS. Brain tissue was removed and post-fixed for 48 h before sectioning and further analysis.

The striatum and mesencephalon were sectioned into 40 μm thick serial sections (Vibratome, Leica). Series of sections regularly spaced were stained with antibodies anti-tyrosine hydroxylase (TH) (sheep polyclonal antibody 1 : 500; Chemicon, Temecula, CA, USA), anti-Iba-1 (rabbit polyclonal antibody 1 : 500; Wako, Chuo-Ku, Osaka, Japan), anti-Cdc42 (mouse monoclonal 1 : 200; Cytoskeleton, Denver, CO, USA), anti-GM130 (mouse monoclonal 1 : 500; Abcam, Cambridge, UK), anti-Cathepsin-D (rabbit polyclonal 1 : 50; Cell Signaling Technology, Danvers, MA). Since Iba-1 staining was incompatible with Cathepsin-D, in order to localize Cathepsin-D in microglial cells, rhodamine-conjugated tomato lectin (Griffonia Simplicifolia Lectin I, 1 : 100, Vector, Burlingame, CA, USA) labeling was performed to detect microglial cells.

Immunohistochemistry and immunofluorescence. *DAB detection.* Sections of the SNpc (40 μm) were used for immunohistochemistry to detect specific cells and structures. Endogenous peroxidase activity was inhibited with 0.3% H_20_2, and non-specific Fc binding sites were blocked with 10% horse serum. The sections were incubated for 48 h (room temperature, constant shaking) with primary antibody (see above) diluted in PBS containing 1% horse serum, 0.5% Triton X-100, and 0.1% sodium azide. The sections were incubated for 4 h in secondary antibody diluted in antibody solution. Binding of antibody was detected with avidin-biotin peroxidase ABC kit (Vectastain, Vector Labs). The sections were mounted on gelatin-coated slides and dehydrated in graded ethanol series and xylene before being coverslipped.

Immunofluorescence. For immunofluorescence, 40 μm sections were treated with 0.5% citrate buffer (65°C, with constant shaking) for 30 minutes to maximize antibody penetration into tissue. Non-specific Fc binding sites were blocked with 10% horse serum, and the sections were incubated for 48 h (room temperature, constant

shaking) with primary antibody diluted in PBS containing 1% horse serum, 0.5% Triton X-100, and 0.1% sodium azide. The sections were incubated for 4 h in labeled secondary antibody; after PBS washes, the sections were incubated with DAPI solution (1 : 1,000) in 1X PBS for 30 minutes. Then, the sections were washed, mounted, and examined for quantification of fluorescence (Zeiss Axioplan 2) or using confocal microscopy (Leica DMIRE2). Appropriate secondary antibodies were used: Alexa 488-conjugated, Alexa 594-conjugated or Alexa 647-conjugated (1 : 1,000) (Molecular Probes). For F-actin staining, the sections where incubated with Alexa Fluor 488-phalloidin or 647-phalloidin (1 : 500 in PBS; Molecular Probes) during two hours at room temperature after immunostaining. After washing, the sections were incubated with DAPI solution for 30 minutes. The sections were washed again, mounted and examined by microscopy for normal fluorescence (Zeiss) and analyzed with confocal microscope (DMIRE2, Leica Microsystems, Exton, PA).

Quantification and sterological analysis. The nigrostriatal pathway was defined according to the Mouse Brain Atlas[43]. Quantification of DAB or fluorescently labeled cells in the striatum was performed on coronal sections in series from each animal. The number of cells was estimated with optical fractionator probe using a computer assisted image analysis system with a Zeiss Axioplan 2 microscope controlled connected to a digital camera. The region of interest was traced using the 1.25 x objective. The number of cells was measured in 200 × 200 µm dissectors covering the surface of the analyzed region. Labeled cells were counted using the 40x objective with counting frames throughout the delineated area of the SNpc in each section via the optical fractionator. Four serial sections of the SNpc were used for each staining in mouse brain. Data were expressed as an absolute number of positive cells in each anatomical region analyzed. Results were expressed as the mean ± SEM.

Confocal analysis and 3D rendering. The brain sections were examined using a Leica DMIRE2 confocal microscope with the 63x oil objective and Leica Confocal Software (Leica Microsystems). Series of optical sections were performed determining an upper and lower threshold using the Z/Y position for Spatial Image Series setting. The optical series covered 20 µm of thickness through the tissue with 0.5 µm per optical section. The confocal microscope settings were established and maintained by Leica and local technicians for optimal resolution. For further details see previous publications[44]. Contacts were defined as areas where co-localization of both markers (Iba-1 and TH) occurs between two cells in at least two 0.5-µm-thick optical sections. A thin area of co-localization can be observed between the two fluorophores. Final confocal images can be illustrated as they appear throughout the stack of sections as a simple 0.5-µm layer or as a transparency of all layers merged together. For ubiquitous staining, such as phalloidin or Cdc42, which label all cells, we normally display single optical sections (0.5 µm) to appreciate the cellular details of the tissue. In contrast, when the stack of images (20 µm) was merged in a transparency, the structure of the tissue was difficult, if not impossible, to observe. In those cases, to avoid saturated images and appreciate the details and clusters we substantially reduce the intensity of the scanning laser to avoid over-saturation of the signal. We also show higher magnifications of the separate channels with better detail to demonstrate that the identification of clusters and other details is not due to cross reaction or invasion of the fluorescence from other channels. It is also important to mention that all scanning were made in sequential mode to avoid cross-reactions.

Three-dimensional reconstructions of the stacks of confocal images were rendered in Imaris software (Bitplane Scientific Software. Zurich. Switzerland). Different surface effects were applied in the 3D rendering to show the structures in the real planes. Videos of the rotations and clipping planes were also generated with Imaris and edited in iMovie Software (Apple Inc. Cupertino. CA) for final versions.

Quantification of activated microglia phenotype. Sections of the SNpc were stained with immunofluorescence to observe microglial cells (Iba-1$^+$ cells). The sections were scanned with confocal microscope as described above and terminal microglial tips per microglial cell were quantified along the z-axes. The microglial area and terminal tips were quantified using confocal images of Iba-1. Scanned confocal planes of 0.5 µm containing Iba-1 labeled cells were processed with image software Image-J to obtain a black and white image. The area of 50 microglial cells (occupied by Iba-1) of the SNpc per each animal was measured in these processed images. Similarly, sections were stained for Iba-1 combined with GM130 and the area occupied by GM130 was quantified in Iba-1$^+$ cells using the same method as described for Iba-1. Two different researchers blindly performed all quantifications.

Quantification of intercellular contacts. Intercellular contacts between microglial cells and dopaminergic neurons or fibers were quantified using stereological methods in confocal stacks of images of the SNpc. The number of contacts Iba-1/TH by field was quantified in 0.5 µm single layers of the 20 µm-thick confocal stacks of images. The contacts between microglial cells and dopaminergic neurons were considered when red and green fluorescence collided in a thin yellow area and were classified in four categories: **Pr-Pr**; Contact between microglial process and dopaminergic process, **B-Pr**; Contact between a microglial cell body and dopaminergic process, **Pr-B**; Processes of microglial cells in contact with a the cell body of a dopaminergic neuron, **B-B**; contact between a microglial cell body and a dopaminergic neuron cell body. The number of contacts per dopaminergic fiber (**Pr-Pr** and **B-Pr**) was quantified considering the total number of remaining fibers, quantified by unbiased stereological methods[45]. The number of **B-B** and **Pr-B** contacts per neuron was quantified neuron by neuron along the z plane. The length of the contacts between the processes and neurons was also quantified in the Leica Confocal software. All these parameters (number of contacts, number of dopaminergic fibers and neurons, number of contacts per neuron and the length of the contact) were quantified in 5 dissectors (sample fields) per each single layer of the 20 µm-thick stacks. Two stacks per brain region per animal were analyzed. In mice, the final result for the length of the contacts was the average of at least 50 events recorded per animal.

Detection of MPP$^+$ by HPLC. C57BL6 mice were injected either with saline (n=5), MPTP (n=5), HA-1077 (n=5) or MPTP+HA-1077 (n=5), according to the protocol described above. Two hours after the treatment, the animals were killed by cervical dislocation and the striatum was dissected, rapidly frozen in dry ice and stored at −80°C until analysis. Each sample of the striatum was homogenized in 250 µl of diluent buffer (0.1 M perchloric acid, 2.7 mM EDTA). The MPP$^+$ standards (Sigma Aldrich) were made with increasing concentrations of MPP+ dissolved in diluent buffer. The analysis of the presence of MPP+ was performed using a Shimadzdu HPLC system (UV detector at 285 nm) with a Kromasil 100 C18 reverse phase column (25 × 0.46 cm, Teknokroma). The mobile phase was 0.1 M sulfuric acid, 0.075 M TEA, 10% acetonitrile, pH 2.3.

Statistical analysis. The data are expressed as the mean ± SEM. The statistical analysis was performed using a one-way ANOVA test following a posthoc analysis. The null hypothesis was rejected for a α risk equal to 5%.

1. Neumann, H., Kotter, M. R. & Franklin, R. J. Debris clearance by microglia: an essential link between degeneration and regeneration. *Brain* **132**, 288–295 (2009).
2. Nimmerjahn, A., Kirchhoff, F. & Helmchen, F. Resting microglial cells are highly dynamic surveillants of brain parenchyma in vivo. *Science (New York, N.Y)* **308**, 1314–1318 (2005).
3. Davalos, D. *et al.* ATP mediates rapid microglial response to local brain injury in vivo. *Nature neuroscience* **8**, 752–758 (2005).
4. Koizumi, S. *et al.* UDP acting at P2Y6 receptors is a mediator of microglial phagocytosis. *Nature* **446**, 1091–1095 (2007).
5. Inoue, K., Koizumi, S., Kataoka, A., Tozaki-Saitoh, H. & Tsuda, M. P2Y(6)-Evoked Microglial Phagocytosis. *International review of neurobiology* **85**, 159–163 (2009).
6. Haynes, S. E. *et al.* The P2Y12 receptor regulates microglial activation by extracellular nucleotides. *Nature neuroscience* **9**, 1512–1519 (2006).
7. Fuhrmann, M. *et al.* Microglial Cx3cr1 knockout prevents neuron loss in a mouse model of Alzheimer's disease. *Nature neuroscience* **13**, 411–413 (2010).
8. Cardona, A. E. *et al.* Control of microglial neurotoxicity by the fractalkine receptor. *Nature neuroscience* **9**, 917–924 (2006).
9. Fricker, M. *et al.* MFG-E8 Mediates Primary Phagocytosis of Viable Neurons during Neuroinflammation. *J Neurosci* **32**, 2657–2666 (2012).
10. Koenigsknecht-Talboo, J. & Landreth, G. E. Microglial phagocytosis induced by fibrillar beta-amyloid and IgGs are differentially regulated by proinflammatory cytokines. *J Neurosci* **25**, 8240–8249 (2005).
11. Ueyama, T. *et al.* Superoxide production at phagosomal cup/phagosome through beta I protein kinase C during Fc gamma R-mediated phagocytosis in microglia. *J Immunol* **173**, 4582–4589 (2004).
12. Majumdar, A. *et al.* Activation of microglia acidifies lysosomes and leads to degradation of Alzheimer amyloid fibrils. *Molecular biology of the cell* **18**, 1490–1496 (2007).
13. Peri, F. & Nusslein-Volhard, C. Live imaging of neuronal degradation by microglia reveals a role for v0-ATPase a1 in phagosomal fusion in vivo. *Cell* **133**, 916–927 (2008).
14. Sierra, A. *et al.* Microglia shape adult hippocampal neurogenesis through apoptosis-coupled phagocytosis. *Cell stem cell* **7**, 483–495 (2010).
15. Welch, M. D. & Mullins, R. D. Cellular control of actin nucleation. *Annual review of cell and developmental biology* **18**, 247–288 (2002).
16. Ridley, A. J. & Hall, A. The small GTP-binding protein rho regulates the assembly of focal adhesions and actin stress fibers in response to growth factors. *Cell* **70**, 389–399 (1992).
17. Ridley, A. J., Paterson, H. F., Johnston, C. L., Diekmann, D. & Hall, A. The small GTP-binding protein rac regulates growth factor-induced membrane ruffling. *Cell* **70**, 401–410 (1992).
18. Kozma, R., Ahmed, S., Best, A. & Lim, L. The Ras-related protein Cdc42Hs and bradykinin promote formation of peripheral actin microspikes and filopodia in Swiss 3T3 fibroblasts. *Molecular and cellular biology* **15**, 1942–1952 (1995).
19. Nobes, C. D. & Hall, A. Rho, rac, and cdc42 GTPases regulate the assembly of multimolecular focal complexes associated with actin stress fibers, lamellipodia, and filopodia. *Cell* **81**, 53–62 (1995).
20. Etienne-Manneville, S. Cdc42--the centre of polarity. *Journal of cell science* **117**, 1291–1300 (2004).
21. May, R. C. & Machesky, L. M. Phagocytosis and the actin cytoskeleton. *Journal of cell science* **114**, 1061–1077 (2001).
22. Etienne-Manneville, S. & Hall, A. Rho GTPases in cell biology. *Nature* **420**, 629–635 (2002).
23. Goodridge, H. S. *et al.* Activation of the innate immune receptor Dectin-1 upon formation of a 'phagocytic synapse'. *Nature* **472**, 471–475 (2011).
24. Tremblay, M. E. *et al.* The Role of Microglia in the Healthy Brain. *J Neurosci* **31**, 16064–16069 (2011).

25. McGeer, P. L., Itagaki, S., Boyes, B. E. & McGeer, E. G. Reactive microglia are positive for HLA-DR in the substantia nigra of Parkinson's and Alzheimer's disease brains. *Neurology* **38**, 1285–1291 (1988).
26. Mueller, B. K., Mack, H. & Teusch, N. Rho kinase, a promising drug target for neurological disorders. *Nature reviews* **4**, 387–398 (2005).
27. Shimizu, Y. *et al.* ROCK-I regulates closure of the eyelids and ventral body wall by inducing assembly of actomyosin bundles. *The Journal of cell biology* **168**, 941–953 (2005).
28. Wilkinson, S., Paterson, H. F. & Marshall, C. J. Cdc42-MRCK and Rho-ROCK signalling cooperate in myosin phosphorylation and cell invasion. *Nature cell biology* **7**, 255–261 (2005).
29. Kim, J. V. & Dustin, M. L. Innate response to focal necrotic injury inside the blood-brain barrier. *J Immunol* **177**, 5269–5277 (2006).
30. Galambos, R. A glia-neural theory of brain function. *Proceedings of the National Academy of Sciences of the United States of America* **47**, 129–136 (1961).
31. Lin, H. H. *et al.* The macrophage F4/80 receptor is required for the induction of antigen-specific efferent regulatory T cells in peripheral tolerance. *The Journal of experimental medicine* **201**, 1615–1625 (2005).
32. Neher, J. J. *et al.* Inhibition of microglial phagocytosis is sufficient to prevent inflammatory neuronal death. *J Immunol* **186**, 4973–4983 (2012).
33. McAllister, A. K. & van de Water, J. Breaking boundaries in neural-immune interactions. *Neuron* **64**, 9–12 (2009).
34. Kokovay, E. & Cunningham, L. A. Bone marrow-derived microglia contribute to the neuroinflammatory response and express iNOS in the MPTP mouse model of Parkinson's disease. *Neurobiology of disease* **19**, 471–478 (2005).
35. Rodriguez, M. *et al.* Bone-marrow-derived cell differentiation into microglia: a study in a progressive mouse model of Parkinson's disease. *Neurobiology of disease* **28**, 316–325 (2007).
36. Reale, M. *et al.* Peripheral cytokines profile in Parkinson's disease. *Brain, behavior, and immunity* **23**, 55–63 (2009).
37. Hamza, T. H. *et al.* Common genetic variation in the HLA region is associated with late-onset sporadic Parkinson's disease. *Nature genetics* **42**, 781–785 (2010).
38. Langston, J. W. *et al.* Evidence of active nerve cell degeneration in the substantia nigra of humans years after 1-methyl-4-phenyl-1,2,3,6-tetrahydropyridine exposure. *Annals of neurology* **46**, 598–605 (1999).
39. Barcia, C. *et al.* Evidence of active microglia in substantia nigra pars compacta of parkinsonian monkeys 1 year after MPTP exposure. *Glia* **46**, 402–409 (2004).
40. Hirsch, E. C. & Hunot, S. Neuroinflammation in Parkinson's disease: a target for neuroprotection? *Lancet neurology* **8**, 382–397 (2009).
41. Ouchi, Y. *et al.* Microglial activation and dopamine terminal loss in early Parkinson's disease. *Annals of neurology* **57**, 168–175 (2005).
42. Gerhard, A. *et al.* In vivo imaging of microglial activation with [11C](R)-PK11195 PET in idiopathic Parkinson's disease. *Neurobiology of disease* **21**, 404–412 (2006).
43. Paxinos, G.a.W., C & Franklin, K. B. J. *The mouse brain in stereotaxic coordinates* (Academic Press, New York, 2001).
44. Barcia, C. *et al.* IFN-gamma signaling, with the synergistic contribution of TNF-alpha, mediates cell specific microglial and astroglial activation in experimental models of Parkinson's disease. *Cell death & disease* **2**, e142 (2011).
45. Gundersen, H. J. Stereology of arbitrary particles. A review of unbiased number and size estimators and the presentation of some new ones, in memory of William R. Thompson. *Journal of microscopy* **143**, 3–45 (1986).

Acknowledgments

This work was supported through grants from: the Spanish Ministry of Competitiveness (SAF2010-21274, SAF2007-062262, FIS PI10-02827 and RYC-2010-06729), *Fundación Séneca* (FS/15329/PI/10) and CIBERNED (*Centro de Investigación Biomédica en Red sobre Enfermedades Neurodegenerativas*). The authors would like to thank all the personnel from the SAI (Servicio de Apoyo a la Investigación) for the help provided at the University of Murcia, particularly María García.

Author contributions

CB designed and performed the research, analyzed the data and wrote the paper. CMR and AG contributed to the immunohistochemistry techniques and data analysis. VA performed the western inmuno-blot and Rho-associated activity assays. MAC performed the HPLC measurements. FRB, CMR, JEY, CMC, VDP and EF contributed to the research, data analysis, and animal care, and MTH contributed to editing the paper.

Additional information

Supplementary information accompanies this paper at http://www.nature.com/scientificreports

Competing financial interests: The authors declare no competing financial interests.

How to cite this article: Barcia, C. *et al.* ROCK/Cdc42-mediated microglial motility and gliapse formation lead to phagocytosis of degenerating dopaminergic neurons *in vivo*. *Sci. Rep.* **2**, 809; DOI:10.1038/srep00809 (2012).